

AN X-RAY PULSAR IN THE OXYGEN-RICH SUPERNOVA REMNANT G292.0+1.8

JOHN P. HUGHES¹, PATRICK O. SLANE², SANGWOOK PARK³, PETER W. A. ROMING³, AND DAVID
 N. BURROWS³

Received _____; accepted _____

ABSTRACT

We report the discovery of pulsed X-ray emission from the compact object CXOU J112439.1–591620 within the supernova remnant (SNR) G292.0+1.8 using the High Resolution Camera on the *Chandra X-ray Observatory*. The X-ray period ($P = 0.13530915$ s) is consistent with extrapolation of the radio pulse period of PSR J1124–5916 for a spindown rate of $\dot{P} = 7.6 \times 10^{-13}$ s/s. The X-ray pulse is single peaked and broad with a FWHM width of $0.23P$ (83°). The pulse-averaged X-ray spectral properties of the pulsar are well described by a featureless power law model with an absorbing column density $N_H = 3.1 \times 10^{21}$ cm⁻², photon index $\Gamma = 1.6$, and unabsorbed 0.3–10 keV band luminosity $L_X = 7.2 \times 10^{32}$ erg s⁻¹. We plausibly identify the location of the pulsar’s termination shock. Pressure balance between the pulsar wind and the larger synchrotron nebula, as well as lifetime issues for the X-ray-emitting electrons, argues for a particle-dominated PWN that is far from the minimum energy condition. Upper limits on the surface temperature of the neutron star are at, or slightly below, values expected from “standard” cooling curves. There is no optical counterpart to the new pulsar; its optical luminosity is at least a factor of 5 below that of the Crab pulsar.

Subject headings: ISM: individual (SNR G292.0+1.8, MSH 11–54) – pulsars: individual (PSR J1124–5916) – stars: neutron – supernova remnants – X-rays: individual (CXOU J112439.1–591620)

1. INTRODUCTION

The composition of the ejecta seen in a supernova remnant (SNR) can be used to constrain the nature of the supernova (e.g., core collapse or thermonuclear) and, in the case of a core collapse SN, estimate a range for the mass of the progenitor star (e.g., Hughes & Singh 1994). Recent studies of the SNR Cas A with *Chandra* and *XMM-Newton* (e.g., Hughes et al. 2000; Bleeker et al. 2001; Willingale et al. 2002) highlight the great potential of the new observatories for such studies. Unfortunately, most SNRs that harbor young pulsars are virtually useless for such investigations: they do not show much evidence for shocked ejecta (e.g., the Crab and 3C 58), are too distant for detailed study (e.g., SNR E0540–69.3 and N157B), or are so evolved that the ejecta cannot be easily distinguished from shocked interstellar gas (e.g., Vela and W44). G292.0+1.8 differs from nearly all other pulsar/SNR associations by virtue of showing spectacular evidence for newly synthesized oxygen-, neon-, and magnesium-rich ejecta (optical: Murdin & Clark 1979; X-ray: Park et al. 2002); having a dynamically determined age (~ 2000 yrs; Murdin & Clark 1979); and being relatively nearby (~ 6 kpc; Gaensler & Wallace 2003). With G292.0+1.8 we have the opportunity to tie information on the progenitor star derived from nucleosynthesis (Park et al. 2003, in prep.) to the origin and evolution of pulsars and their wind nebulae (PWNe).

Recently *Chandra* revealed an X-ray point source (CXOU J112439.1–591620) centered on a diffuse synchrotron nebula in G292.0+1.8 (Hughes et al. 2001). In a follow-up study Camilo et al. (2002) discovered a 135-ms young pulsar within or near G292.0+1.8 using the Parkes

radio telescope that is almost surely the counterpart to the *Chandra* point source. However the large beam of the Parkes telescope ($\sim 14'$ FWHM) means that the case is not ironclad. Here we report on high temporal and spatial resolution X-ray observations in which we detect the pulsed signal from CXOU J112439.1–591620, clearly identifying it as the compact remnant of the SN that formed G292.0+1.8.

2. X-RAY PULSAR

We observed SNR G292.0+1.8 beginning on 14 July 2001 using the *Chandra* High Resolution Camera (HRC) in timing mode with the pulsar candidate at the aimpoint (ObsID 1953). Timing mode observations utilize the central portion of the HRC-S focal plane array which provides a field of view roughly $6'$ by $30'$. Individual photons are time tagged to an accuracy of about $16 \mu\text{s}$; we corrected photon arrival times to the solar-system barycenter using the position of the pulsar candidate. Our observation was nearly continuous; the only interruptions were 8 gaps of ~ 2 s duration each, distributed throughout the exposure. The livetime corrected exposure was 49578 s.

Figure 1 (left panel) shows a roughly $6'' \times 6''$ portion of the HRC image containing the pulsar candidate at position R.A. = 11:24:39.1, decl. = $-59:16:20$ (J2000). There is an unresolved source centered on a small, diffuse, elliptically-shaped nebula. Within a radius of $2''$ (15 HRC pixels) of the point source we detected 1324 X-ray photons. First we carried out a blind search for pulsations on these events. Light curves were constructed for the entire duration of the observation using four different binsizes of 0.0237563 s, 0.0118781 s, 0.00593907 s, and 0.00296954 s corresponding

¹ Department of Physics and Astronomy, Rutgers University, 136 Frelinghuysen Road, Piscataway, NJ 08854-8019; jph@physics.rutgers.edu

² Harvard-Smithsonian Center for Astrophysics, 60 Garden Street, Cambridge, MA 02138; slane@head-cfa.harvard.edu

³ Department of Astronomy and Astrophysics, Pennsylvania State University, 525 Davey Laboratory, University Park, PA. 16802

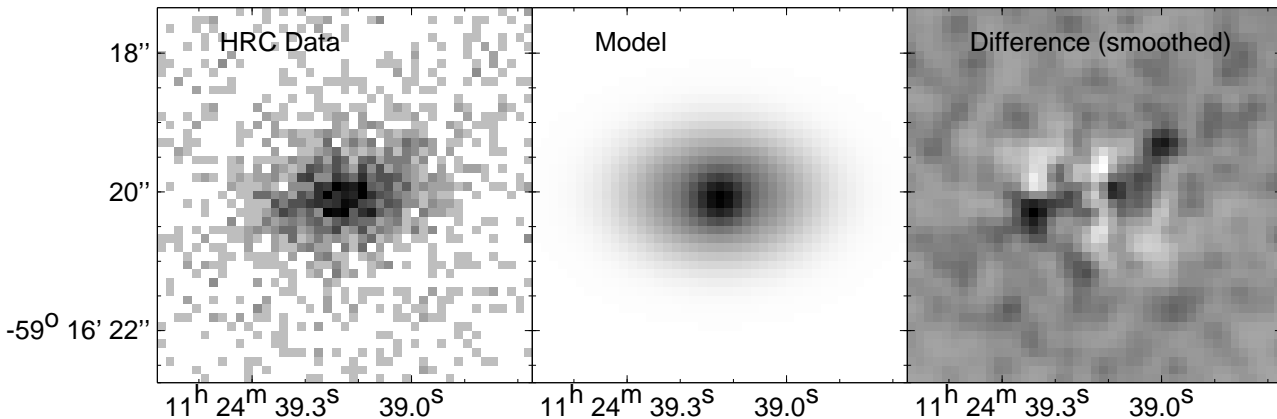


FIG. 1.— A portion of the *Chandra* high resolution camera image centered on CXOU J112439.1–591620. In the left and middle panels the grayscale is linear from 0 to 15 HRC counts per pixel ($0.1318''$ square). In the right panel the linear grayscale extends from -1.4 to 1.8 counts per pixel. This last image was smoothed with a 1 pixel σ gaussian kernel. Coordinates are given in epoch J2000.

to 2^{21} , 2^{22} , 2^{23} , and 2^{24} temporal bins. A coherent FFT of the entire light curve showed no statistically significant pulsed signal for any of these cases. The distribution of Fourier powers was consistent with noise and the individual peak Fourier powers obtained were 30.4, 31.9, 32.9, and 34.2 for the four cases, respectively, none of which are statistically significant. As a verification of our methods and IDL software we applied the same programs to the HRC data of PSR B0540–69.3, observed on 22 June 2000 (ObsID 1745) using the same configuration as our data. The pulsar was easily detected at a frequency of 19.7941 Hz with a peak Fourier power of 50.3 (99.998% significance).

A much more sensitive search for X-ray pulsations is possible by narrowing the range of trial frequencies to be consistent with the radio pulse and a reasonable range of \dot{P} values. We employed the Z_n^2 test (Buccheri et al. 1983) which applies a harmonic analysis to the phases of photon arrival times for a given trial pulsation frequency. One advantage of the method, compared to epoch-folding for example, is that it requires no binning. Another is that, even for as few as 100 detected photons, the statistic is distributed like χ^2 with $2n$ degrees of freedom. In our searches we use $n = 2$.

We searched eleven trial frequencies spaced by $\Delta f = 1 \times 10^{-5}$ Hz (roughly the frequency resolution of our data) and centered on the expected value based on extrapolating the radio ephemeris to the midpoint of the HRC observation (MJD = 52105.18). The peak Z_2^2 value was 22.6 corresponding to the 99.8% significance level. The search was refined by reducing Δf to 2×10^{-6} Hz and again searching eleven trial frequencies, this time centered on the most likely previous pulsation frequency. This iteration yielded a peak Z_2^2 value of 27.9 (99.97% significant or approximately 3.6σ) at a period of 0.13530915 s. The period error (4×10^{-8} s, 1σ) was determined using a bootstrap algorithm. In Table 1 we quote observed properties of the X-ray pulsar. By comparing our pulse period to the value obtained by Camilo et al. (2002) roughly two months later we derive a period derivative of $\dot{P} = 7.62 \pm 0.06 \times 10^{-13}$ s/s that differs by $\sim 2.5 \sigma$ from the value quoted in the radio discovery paper. At present we do not know the relative

X-ray and radio pulse phases and, due to apparent rotational instabilities in the neutron star, it is not possible to extrapolate the radio ephemeris from September 2001 back to July 2001 accurately enough to measure relative phases.

As an additional check on the detection of pulsed X-ray emission, we applied the last search iteration to the first and second halves of the data set (split in time) independently. The pulse was detected in each half at the appropriate Z_2^2 value and pulsation frequency and with similar light curve shapes.

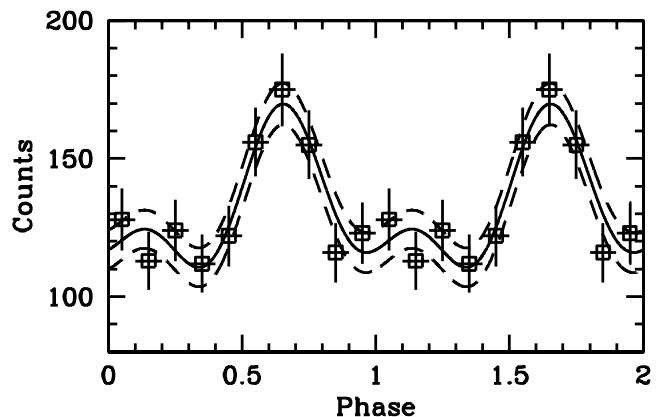


FIG. 2.— Pulse phase light curve for PSR J1124–5916 folded modulu the best-fit period of 0.13530915 s. Two complete periods are shown. Note the suppressed zero on the y-axis. Also plotted are the Fourier series estimator (de Jager, Swanepoel, & Raubenheimer 1986) of the light curve (solid curve) and its 1σ uncertainty (dashed curves).

The pulse in the X-ray band is single peaked and symmetric (see Fig. 2), similar to the radio pulse, although the X-ray pulse width (FWHM $\sim 0.23P \sim 83^\circ$) is somewhat broader than the radio one. The smooth curve in figure 2 is a Fourier series estimate (de Jager, Swanepoel, & Raubenheimer 1986) of the light curve employing two harmonics. If we assume the pulse extends over phase bins 0.43–0.90, we determine the fraction of pulsed X-rays in the $2''$ radius extraction region to be $11 \pm 1\%$. This includes contribution from the diffuse compact nebula, which we quantify next.

TABLE 1
PROPERTIES OF X-RAY PSR J1124–5916

Parameter	Value
R.A. (J2000)	11 24 39.1
Decl. (J2000)	−59 16 20
Period, P (s)	0.13530915(4)
Epoch (MJD)	52105.18
Observation span (hr)	14.3
FWHM of pulse	$\sim 0.23P$
Pulsed fraction (%)	91^{+9}_{-24}
HRC rate (s^{-1})	0.0032(8)
Column density, N_{H} (cm^{-2})	$3.1(4) \times 10^{21}$
Photon index, Γ	1.6(1)
Luminosity, L_X (0.3–10 keV) (erg s^{-1}) (Unabsorbed)	$7.2 \times 10^{32} (D/6 \text{ kpc})^2$

Note.—Numbers in parentheses represent 1σ uncertainties in the least significant digits quoted.

3. EXTENDED COMPACT NEBULA

Shown in the middle panel of figure 1 is our best fit spatial model for the HRC data: an unresolved point source (i.e., a gaussian whose best-fit angular size is consistent with the *Chandra* PSF) and an elliptical gaussian with a FWHM of $1.8''$ (along the major axis) and an axial ratio of 2. In this model the point source contains 160 ± 40 X-ray events while the extended elliptical component contains 1440 events. Compared to the number of pulsed events we detect (146 ± 13), it is clear that the point source itself is highly pulsed with a pulsed fraction of $>65\%$ in the HRC band.

The rightmost panel in Figure 1 shows the difference between the HRC data and the best-fit image model. There is good evidence for excess X-ray emission above that given by the model, to either side of the point source and oriented generally in the SE-NW direction. One possibility is that the excess emission comes from a pair of jets. This feature is nearly aligned with the direction from the current position of the point source back toward the center of the SNR (toward the NW), which would indicate aligned spin axis and proper motion directions for PSR J1124–5916, as seen in the Crab and Vela pulsars. On the other hand, it is also possible that the excess emission arises from a toroidal structure in the nebula (like the torus in the Crab Nebula) seen in projection. In this scenario the torus would be nearly aligned with the major axis of the compact nebula. By analogy to the Crab and its pulsar, we would therefore expect that the spin axis to be perpendicular to the long axis of the compact nebula (i.e., aligned NE-SW). This would put the pulsar’s spin axis nearly perpendicular to its proper motion direction. The current *Chandra* data do not allow us to discriminate between these possibilities.

The extended compact nebula is the only emission feature in the PWN within an arcmin or so of the pulsar and therefore is the only plausible candidate for the pulsar wind termination shock. If we interpret the edge of the nebula with the location of this shock, we can then estimate the confining pressure (i.e., in the PWN) necessary

to balance the ram pressure of the wind, $P_w = \dot{E}/4\pi cr_w^2$, assuming spherical symmetry. The mean radius of the compact nebula is $0.036 d_6$ pc and the spin down energy loss of the pulsar is $\dot{E} = 1.2 \times 10^{37} \text{ erg s}^{-1}$ (Camilo et al. 2002), so the pressure is $P_w = 2.6 \times 10^{-9} d_6^{-2} \text{ erg cm}^{-3}$.

We estimate the pressure in the PWN from the properties of the radio emission, which we take from Gaensler & Wallace (2003), and the theory of synchrotron emission (Longair 1994). Under the minimum energy condition we find that $P_{\text{PWN,min}} \sim 1.3 \times 10^{-10} d_6^{-4/7} \text{ erg cm}^{-3}$ assuming equal energy densities in the protons and electrons and a volume filling factor of unity. The average nebular magnetic field under these conditions is $B_{\text{min}} \sim 48 d_6^{-2/7} \mu\text{G}$, which implies a very short synchrotron lifetime, $t \sim 140 d_6^{3/7} (h\nu/2 \text{ keV})^{-1/2} \text{ yr}$, for the electrons giving rise to the X-ray emission. Such a short lifetime is inconsistent with the observation that the X-ray synchrotron nebula covers as large an extent as the radio nebula does.

A possible solution to these discrepancies lies in relaxing the minimum energy condition. If we move in the direction of a smaller mean nebular magnetic field we resolve the lifetime issue. A magnetic field strength of $\lesssim 8 \mu\text{G}$ would ensure that the X-ray synchrotron cooling time is $\gtrsim 2000 \text{ yr}$. In order that the pressure in the synchrotron nebula be sufficiently strong to balance the ram pressure of the pulsar’s wind requires a value of $B \sim 3 \mu\text{G}$. The total energy in the nebula would then be $\sim 4 \times 10^{49} \text{ ergs}$, contained nearly entirely in particles. Since this energy has come from the spin-down of the pulsar, it sets a constraint on the initial spin period: $P_0 \sim 22 \text{ ms}$ for a canonical NS momentum of inertia of $I \equiv 10^{45} \text{ g cm}^2$. This P_0 value is considerably less than the value of $\sim 90 \text{ ms}$ estimated by Camilo et al. (2002). The simplest way to accommodate our low value for the initial spin period would be to increase the true age of the pulsar to $\sim 2800 \text{ yr}$ or more.

It is important to note that neither the magnetic field nor the pressure is expected to be uniform in PWNe, as we assumed in the calculations above. In the Kennel & Coroniti (1984) model for the Crab Nebula the total pressure is greatest at the termination shock and then falls by factors of 3–10 at larger radii. In addition, equipartition between particles and fields is attained only at a significant distance from the pulsar; near the termination shock the magnetic field is low and the pressure is particle-dominated. Because of the higher central pressure, we expect the volume-averaged magnetic field under this model to be somewhat larger than that estimated above, which would have the effect of relaxing the energetics constraint on the pulsar’s initial spin period. Our apparent need for a particle-dominated PWN in G292.0+1.8 is suggestive of a low value for the magnetization parameter in the context of this model. We note, however, that interaction between the reverse shock and the PWN (which has not yet been conclusively established) may offer an alternate explanation for why the nebula is far from the minimum energy condition. Further study of these issues, although beyond the scope of our work here, is clearly warranted.

4. NEUTRON STAR COOLING

The NS in G292.0+1.8 is quite young with a most likely age range of ~ 2000 yrs to ~ 2900 yrs, corresponding to the free expansion age of the O-rich knots and the pulsar characteristic age, respectively. According to NS cooling models (e.g., Tsuruta 1998; Page 1998), the surface temperature at this age should be high enough to produce detectable X-ray emission. As shown by Hughes et al. (2001), the ACIS-S spectrum of the pulsar is fully consistent with a single absorbed power-law. Here we determine the upper limit to the intensity of an additional blackbody spectral component as a function of its temperature, T_{BB} . We utilized two independent spectra extracted from the CTI-corrected data (Park et al. 2002): one from a 3×3 pixel ($1.5'' \times 1.5''$) region centered on the pulsar, and another, comprising the diffuse nebula, from an ellipse of size 7×11 pixels ($3.4'' \times 5.4''$) excluding the central pulsar region. The pulsar spectrum was fit to the sum of a blackbody and a power-law model including absorption, while the nebular spectrum was fit to an absorbed power-law model alone. This latter spectrum served as an independent constraint on the column density, which was constrained to be the same between the two spectra. For reference, table 1 lists pure power-law spectral parameters for the pulsar.

For a given fixed value of T_{BB} , the ACIS-S data set an upper limit on the allowed normalization (or flux) of the blackbody component. One can express the normalization limit in terms of the square of the ratio of the blackbody emitter's radius to its distance. The 3σ limit on this ratio as a function of T_{BB} is plotted in figure 3.

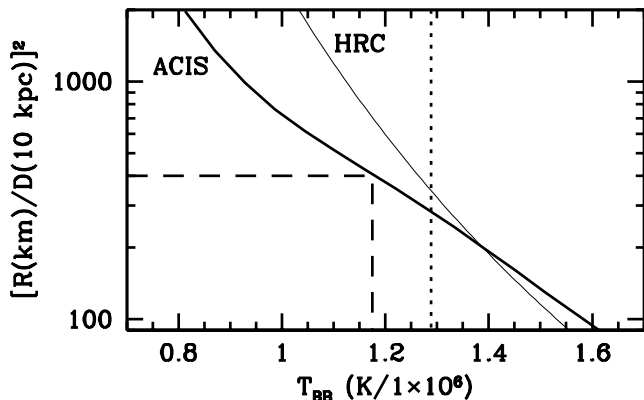


FIG. 3.— Constraint on the normalization of a blackbody spectral component vs. its temperature from fits to the time-averaged ACIS-S spectrum of PSR J1124–5916 (thick solid curve). The thin solid curve indicates the constraint based on the unpulsed HRC count rate of the X-ray pulsar. The allowed region lies to the left and below the curves shown. The dashed lines show the temperature constraint for the nominal value of distance to G292.0+1.8 (6 kpc) and a 12 km radius NS. The vertical dotted line shows the temperature expected for a standard NS cooling curve.

Since the ACIS-S spectrum is consistent with an entirely nonthermal origin, the pulsed emission seen in the HRC, which comprises $>65\%$ of the total HRC rate from the pulsar, therefore must be dominated by nonthermal, i.e., magnetospheric, emission as well. The unpulsed HRC emission, however, can be used to set another constraint on the mean surface temperature of the NS. We convert the 3σ upper limit on the unpulsed HRC count rate ($2.8 \times 10^{-3} \text{ s}^{-1}$), assuming the 3σ upper limit on the column density to the pulsar ($N_H = 4.75 \times 10^{21} \text{ atom cm}^{-2}$, derived

from the nebular spectrum) to a constraint on the blackbody normalization as a function of T_{BB} . This constraint, which is fully consistent with the one from the ACIS-S spectral analysis, is shown as the thin curve in figure 3.

Recent work (Gaensler & Wallace 2003) suggests that the distance to G292.0+1.8 is ~ 6 kpc. Using this value and assuming a 12 km radius for the NS, we obtain a constraint of $T_{BB} < 1.18 \times 10^6 \text{ K}$ on the surface temperature of the NS. The expected temperature, assuming standard NS cooling models, is $1.28 \times 10^6 \text{ K}$ (Page 1998). Although this is suggestive of the presence of exotic cooling processes, systematic uncertainties make this result less secure than the recent result on the apparent need for exotic cooling processes for the NS in 3C 58 (Slane, Helfand, & Murray 2002). The NS in G292.0+1.8 would be consistent with standard cooling if it were as distant as 7 kpc, or if the compact star's radius were as small as 10 km. On the other hand pure blackbody spectral models tend to overpredict (by factors of 1.5 or more) the effective temperature of NS surfaces when light element atmospheres are included (Lloyd, Hernquist, & Heyl 2002).

5. LIMITS ON AN OPTICAL COUNTERPART

Optical emission from isolated pulsars within supernova remnants has currently been detected from only four objects: PSR B0531+21 (Crab), PSR B0540–69.3 (in the LMC), PSR B1509–58 (G320.4–1.2), and PSR B0833–45 (Vela) (see, for example, Nasuti et al. 1997 and references therein). The first three are very young pulsars (1000–2000 years old), while the pulsar in Vela is considerably older ($\sim 10,000$ yrs), although it is still rather young compared to the average radio pulsar. Across the optical band these pulsars show flat power-law spectra ($\alpha \sim 0$ for $F_\nu \propto \nu^{-\alpha}$), although their intrinsic luminosity densities (i.e., $L_\nu = 4\pi D^2 F_\nu$) span 5 orders of magnitude from $0.5\text{--}2 \times 10^{19} \text{ erg s}^{-1} \text{ Hz}^{-1}$ (PSR B0531+21, PSR B0540–69.3, and PSR B1509–58) to $3\text{--}6 \times 10^{14} \text{ erg s}^{-1} \text{ Hz}^{-1}$ (PSR B0833–45). In terms of age and remnant optical properties (i.e., the presence of high velocity, oxygen-rich optical emission), G292.0+1.8 most closely resembles SNR 0540–69.3. However in terms of spin-down energy loss ($\sim 10^{37} \text{ erg s}^{-1}$), the pulsar in G292.0+1.8 is more similar to PSR B0833–45 and PSR B1509–58.

With *Chandra* we have localized the G292.0+1.8 pulsar to an absolute position accuracy of $\sim 1''$. Within double this error circle there is no optical counterpart visible in the Digitized Sky Survey. We have obtained an upper limit on optical emission from the pulsar, $B \gtrsim 22$, based on a narrow-band blue continuum image of G292.0+1.8 taken by P.F. Winkler and K.S. Long from the CTIO 4-m in 1991. This corresponds to an intrinsic luminosity density of $L_\nu < 3 \times 10^{18} \text{ erg s}^{-1} \text{ Hz}^{-1}$ (assuming a distance of 6 kpc and extinction of $A_B \sim 2.3$). This is about an order of magnitude less than the optical emission of the Crab and SNR 0540–69.3 pulsars, but is only about a factor of two less than the optical emission from PSR B1509–58 (Caraveo, Mereghetti, & Bignami 1994). A considerably fainter upper limit, based on data acquired at CTIO in April 2002, will be the subject of a forthcoming article.

We are grateful to Fernando Camilo and Bryan Gaensler for sharing results or data prior to publication and

to Frank Winkler for supplying the optical image of G292.0+1.8. Mike Juda gave us some helpful advice regarding the HRC data. We thank Karen Lewis and John Nousek for their help with the initial proposal for HRC

time. We also thank Simon Johnston for his useful comments as referee. Partial support for this research was provided by *Chandra* grant GO1-2052X to JPH.

REFERENCES

- Buccheri, R., et al. 1983, *A&A*, 128, 245
 Camilo, F., Manchester, R. N., Gaensler, B. M., Lorimer, D. R., Sarkissian, J. 2002, *ApJ*, 567, L71
 Caraveo, P. A., Mereghetti, S., & Bignami, G. F. 1994, *ApJ*, 423, L125
 De Jager, O. C., Swanepoel, J. W. H., & Raubenheimer, B. C. 1986, *A&A*, 170, 187
 Gaensler, B. M., & Wallace, B. J. 2003, *ApJ*, in press (astro-ph/0305168)
 Hughes, J. P., Slane, P. O., Burrows, D. N., Garmire, G. P., Nousek, J. A., Olbert, C. M., & Keohane, J. W. 2001, *ApJ*, 559, L153
 Kennel, C. F., & Coroniti, F. V. 1984, *ApJ*, 283, 694
 Longair, M. S. 1994, *High Energy Astrophysics*, Vol 2, 2nd edition (Cambridge: Cambridge University Press) p. 292ff
 Murdin, P., & Clark, D. H. 1979, *MNRAS*, 189, 501
 Nasuti, F. P., Mignani, R., Caraveo, P. A., & Bignami, G. F. 1997, *A&A*, 323, 839
 Page, D. 1998, in *The Many Faces of Neutron Stars*, ed. R. Buccheri, J. van Paradijs, & M. A. Alpar (Dordrecht: Kluwer), 539
 Park, S., Roming, P. W. A., Hughes, J. P., Slane, P. O., Burrows, D. N., Garmire, G. P., & Nousek, J. A. 2002, *ApJL*, 564, L39
 Rees, M. J., & Gunn, J. E. 1974, *MNRAS*, 167, 1
 Slane, P. O., Helfand, D. J., & Murray, S. S. 2002, *ApJ*, 571, L45
 Tsuruta 1998, *Rev. Mod. Phys.*